Eleventh International Conference on Computational Fluid Dynamics (ICCFD11), Maui, HI, USA, July 11-15, 2022

ICCFD11-2022-2003

CFD Modeling of Droplets Heated by an X-ray Free Electron Laser

C. Parisuaña[*,**], D. C. Eder[***], M. Gauthier[**], C. Schoenwaelder[**], C. A. Stan[****], S. H. Glenzer[**]

Corresponding author: dceder@hawaii.edu

[*]Department of Mechanical Engineering, Stanford University, Stanford, CA, USA.

[**]SLAC National Accelerator Laboratory, Menlo Park, CA, USA

[***]University of Hawai'i at Manōa, HI, USA.

[****]Department of Physics, Rutgers University-Newark, Newark, NJ, USA.

Abstract:

Material in HED regimes are at very high pressures and temperatures but can often still be modeled in the plasma-fluid approximation. Historically HED regimes were created using large laser/ion-beam drivers heating solid targets. Exciting data was obtained from these single shot experiments. In recent years there has been a shift to obtain HED related data from a large number of shots by using high-repetition-rate drivers. For high-repetition-rate experiments a series of droplet targets are often used to have a fresh target/droplet for each shot. However, one must make sure that target debris from the previous shot does not degrade the target for subsequent shots. This is a challenging CFD problem as one needs to model the initial dynamics of the heated droplet and the subsequent interaction with the following droplets. We use the CFD modeling code PISALE to study this complex problem. We discuss results for liquid hydrogen droplets heated by an x-ray free electron laser (XFEL). We first show 2D results for single heated droplet then 3D results for a heated droplet interacting with two unheated droplets.

Keywords: CFD, HED, Droplet Formation and Interaction, high speed flows.

1 Introduction

High-repetition-rate high-intensity short-pulse lasers are responsible for the recent paradigm shift in high energy density (HED) science because they allow going from shots-per-hour experiments to multiple shots-per-second experiments [1]. Statistics, reproducibility, ability to exploit machine learning and robustness of model testing are some of the areas that can be exploited and contribute to accelerate the field. With this shift comes also another one: target availability. Stationary targets are destroyed after their interaction with X-rays. This was not a problem in shot-per-hour experiments because the solution was having many targets ready to replace the damaged one. High-repetition-rate experiments need targets that can withstand multiple shots per second without degradation. Examples of high-rep targets are waterjet targets, cryogenic targets and liquid droplet targets. Droplet targets have been used for laser-driven ion acceleration as spherical free-standing reduced mass targets [2]. The advantage is that they do not need a supporting structure like jet targets that might introduce large perturbations after each shock, but fratricide can be a major issue if droplets are too close to each other or the x-ray free electron laser (XFEL) pulse energy is very high. Experiments using water droplets [3] have shown that debris following the explosion of one droplet affect the nearby droplets. If following droplets are impacted too much, it is possible to skip these droplet but this results in significant reduction of effective repetition rate and hence data collection rate of the system.

This work aims to model the dynamics following the explosion of hydrogen droplet heated by an XFEL pulse and the interaction with other droplets. Hydrogen is suitable for ion-acceleration applications. Hydrogen/deuterium can provide a pure source of protons and deuterons, free from the contaminant ions typically observed [4]. For modeling we use the PISALE (Pacific Island Structured-AMR with ALE) code developed by the University of Hawai'i [5] (see also https://pisale.bitbucket.io/). PISALE combines Arbitrary Lagrangian-Eulerian (ALE) hydrodynamics with Adaptive Mesh Refinement (AMR) and has physics models that include laser/ion deposition, radiation hydrodynamics, thermal diffusion, anisotropic material strength with material time history, advanced models for fragmentation, and includes models for surface tension effects [6].

2 Problem Statement

We model a single hydrogen droplet in 2D and three hydrogen droplets in 3D using the PISALE code. The 2D droplet simulation offers a test case that has higher resolution and less computational running time compared to a 3D simulation, but does not capture the multidroplet problem. On the other hand, the 3D simulation allows modeling multiple droplets -three droplets in our case- and let us study the effect of droplet explosion on nearby droplets. The 2D case simulation results are used to assess the accuracy of the results for the 3D case at early times (0ns - 3ns). Finally, we show that basic dynamic response of hydrogen droplets heated by an XFEL are similar to experimental data of larger water droplets heated by an XFEL [3].

Our initial simulation results shown in this paper do not include surface tension effects. For both hydrogen and water droplets, the effect of surface tension on the dynamics of the droplet heated by the XFEL beam is generally very small but can be important for the following droplets. While the surface tension coefficient for hydrogen is significantly smaller than the coefficient of other materials we have modeled previously, we have not found any reason that the height function approach that we use in PISALE [6] would not be an appropriate choice. We are currently refining the model in PISALE [7] and future simulations will use this surface tension model.

2.1 2D droplet

The 2D hydrogen droplet is modeled using a three-level hierarchy adaptive mesh (see left image in Figure 1). The domain size is x $\in$ [0, 0.25cm], y $\in$ [0, 0.25cm]. The first hierarchy level consists of a grid of 18 000 x 18 000. The second hierarchy level acts on the subdivisions belonging to the first hierarchy level and divides it by a 3x3 grid. The third hierarchy level does the same on the subdivisions belonging to the second hierarchy level. The initial time step is dt = 10^{-12}s and it is increased at most by a factor of 1.05 at each step such that $dt_{new} \leq 1.05\ dt_{old}$. Because of symmetry is only necessary to model 1/4 of the droplet. We ran the simulation on NERSC using 64 cores (2 nodes with 32 tasks per node).

droplet material	droplet radius [μm]	temperature (K)	chamber pressure (Mbar)?
Hydrogen	2.5	18.0	1.33 x 10^{-12}

Table 1: Initial state for hydrogen droplet

The initial value of density is computed using an existing equation-of-state (eos) hydrogen table that is called by PISALE code using as inputs the temperature and chamber pressure values from Table 1. Similarly, the internal energy is computed by using as inputs the temperature from Table 1 and the hydrogen density obtained from the equation-of-state.

H_2 absorption rate (1/cm)	spot energy per H_2 mass (Terg/g)	spot energy per H_2 volume (Terg/cm^3)
0.02870	0.452769	0.036542

Table 2: XFEL pulse absorption into the droplet input values

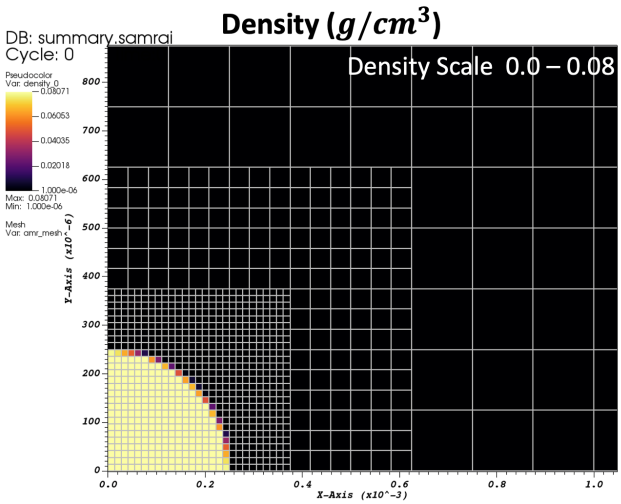

Figure 1: Initial conditions for a 5 micron hydrogen droplet heated by an XFEL beam. The x and y coordinates are in cm. Left image shows the initial density value and the AMR mesh. Right image shows the initial temperature.

X-ray photons are absorbed on subfemtosecond timescales through photoelectric effect [3] [8] [9], so our model assumes that the XFEL pulse heats the droplet isochorically. Table 2 shows the H_2 absorption rate that we use as input in our simulation. This value gives an attenuation length of photons in hydrogen equal to 34.8cm $\gg$ droplet's diameter, and photon energy of $\simeq$3390eV [10]. As a first approximation we can assume that no attenuation has occurred along droplet. Thus, the XFEL pulse heats a filament along the hydrogen droplet and if we also assume that no diffusion has occurred at this timescales, the volume of the heated filament has a cross sectional area of the same size of the X-ray beam [3]. Based on this, we model the XFEL pulse heating by imposing an initial temperature in the region of the droplet where the heating occurs. The XFEL pulse parameters inputs of the simulation are shown in Table 3. The initial conditions for the 2D hydrogen droplet are shown in Figure 1. The left image shows that the initial droplet density is 0.08071 g/cm^3 and that the background density is 1x10^{-6}g/cm^3. The right image shows the initial temperature of the droplet including a hot region with a temperature equivalent to the energy deposited by the XFEL pulse.

laser pulse energy (Terg)	spot radius [μm]	spot fluence (Terg/cm^2)
1.0 x 10^{-8}	0.5	1.27324

Table 3: XFEL pulse parameters for 2D hydrogen droplet PISALE simulation

2.2 3D droplets

The 3D hydrogen droplet is modeled using the same three-level hierarchy adaptive mesh but with some changes. The domain size for this case was reduced to x $\in$ [-0.0075cm, 0.0075cm], y $\in$ [-0.0075cm, 0.0075cm], z $\in$ [-0.0075cm, 0.0075cm], with the first hierarchy level consisting of a smaller grid of 900 x 900. The subdivisions for the second and third hierarchy mesh refinement (3x3x3) and the time step are similar to the 2D case as well as the use of cylindrical symmetry. We increase the number of cores to 128 (4 nodes with 32 tasks per node). We use the same assumptions, model and input values (Tables 1, 2, 3) as in the 2D case. Figure 3 shows the initial conditions for the 3D case. The 5 micron diameter hydrogen droplets are separated by a distance of 5μm. All the droplets have the same initial density value (0.08071 g/cm^3), with the bottom droplet being subjected to heating due to the incoming XFEL beam along the x-axis.

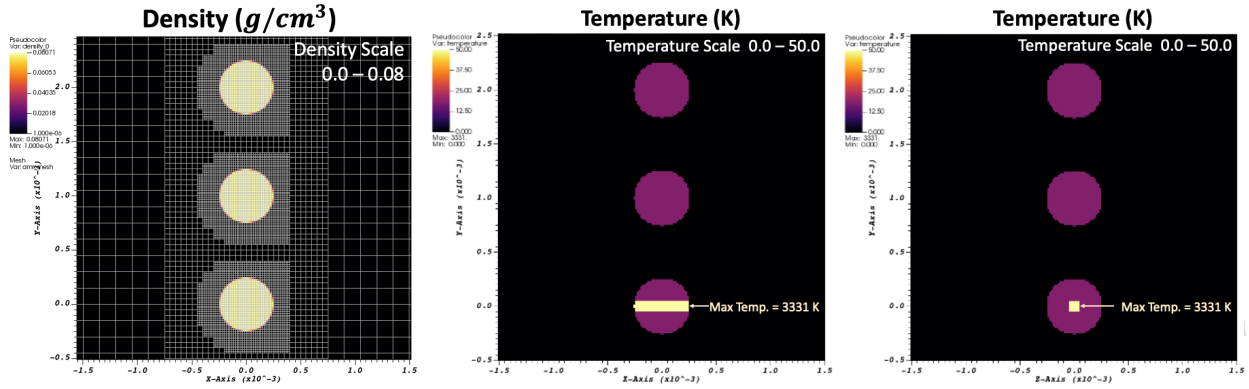

Figure 2: Initial conditions for 3D hydrogen droplets PISALE simulation. Three 5 micron hydrogen droplets with the bottom droplet being heated by an XFEL beam. Left image shows initial density and AMR mesh. Middle image and rightmost image shows the side and inline view of the initial temperature respectively.

3 Results

Figure 3 and Figure 4 show the early time evolution for 2D and 3D cases respectively. We can see that after droplet explosion, the material expands and reaches the second droplet around 3ns. Even though the 3D case uses a smaller domain and resolution, it captures the droplet explosion accurately when compared to the 2D case, which can be seen in Figure 5.

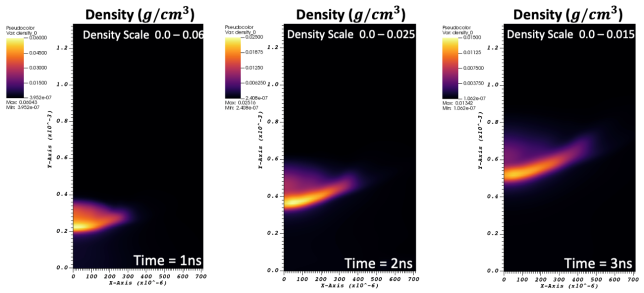

Figure 3: 2D hydrogen droplet density at 1, 2, 3 ns.

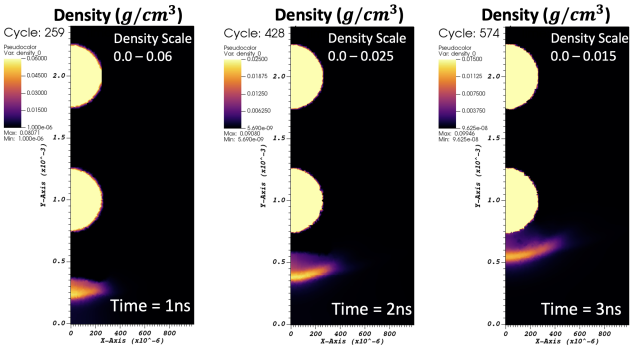

Figure 4: 3D hydrogen droplets density at 1, 2, 3 ns.

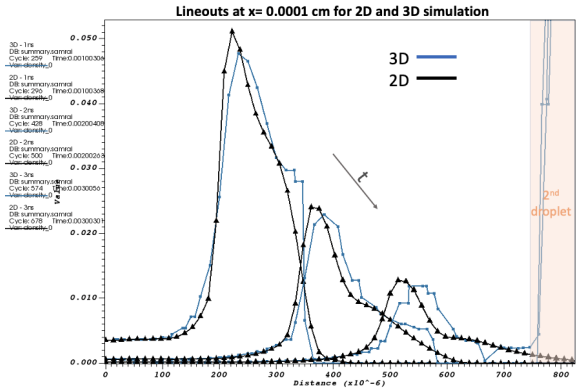

Figure 5: 2D vs 3D density curves for 1, 2 and 3ns. Lineouts were extracted at x=0.0001cm.

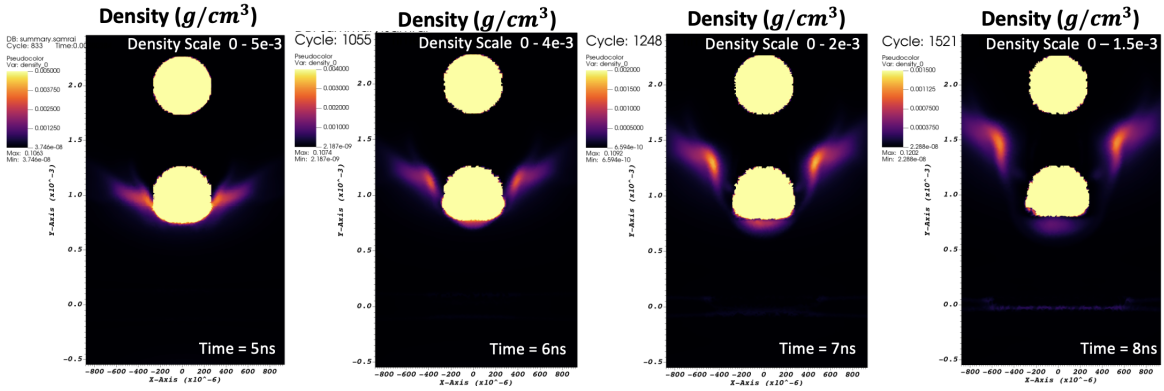

Figure 6: Time evolution of density for 3D hydrogen droplets at 5, 6, 7 and 8ns.

Figure 6 shows the time evolution of 3D case when the debris following the droplet explosion starts interacting with the second droplet. For times $\geq$ 6ns, the change in shape at the bottom edge of the second droplet is evident. This change in shape can be attributed to heat and momentum exchange between the second droplet and the material ejected. For a particular high repetition rate setup we usually want to keep the same conditions shot after shot if the goal is to do statistics. Thus, the second droplet would become a non-ideal target because it does not have the same conditions (temperature, density, pressure, size) as the first one. On one hand, the proximity of the second droplet to the first one limits the high-rep of droplet targets. On the other hand, the second droplet shields debris coming from the explosion of the first droplet that otherwise would have reached the third droplet quicker. This opens an interesting question on how to optimize this target, should we send trains of droplets to protect the next batch or is it better to simply increase the distance between droplets?

The three-dimensional dynamics of droplet explosions for hydrogen droplets simulations (left) and water droplets experimental measurements (right) can be seen in Figures 7 and 8. Note that the separation between the smaller hydrogen droplets is different to the larger water droplets. The ratio of the distance between water droplets and their diameter is 2:1 while the same ration for the hydrogen droplets simulation is 1:1.

Figure 7 shows the side view of the hydrogen droplets after droplet explosion and on the right we show the same view for Stan et al. water droplets experimental data [3]. We see that in our simulation on the left, the shockwave front structure is very similar to the one in the experimental data. Furthermore, in both of them we appreciate high density areas near the shockwave fronts and a lower density region as we depart from them. Figure 8 shows the inline view following the droplet explosion. The left image corresponds to the

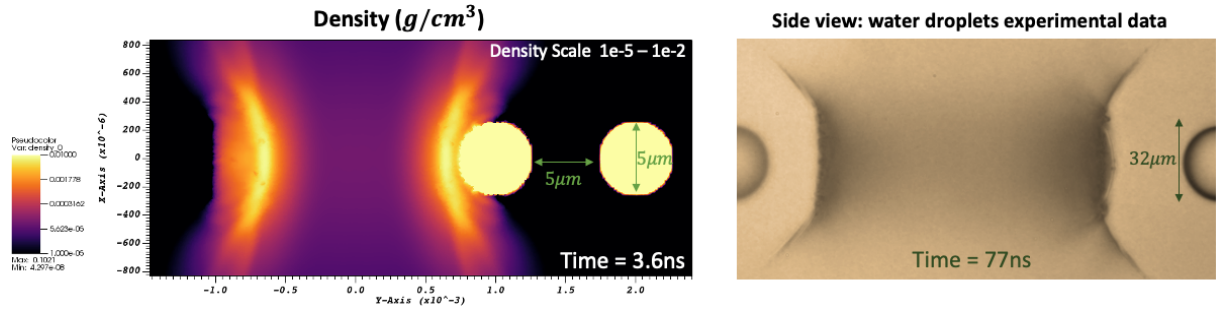

Figure 7: Side view of 3D droplets. Left image shows z-plane projection of 5-μm-diameter hydrogen droplets after 3.6ns of the XFEL-droplet interaction, laser pulse energy of 1mJ. Right image shows experimental data of 32-μm-diameter water droplets, 1 $\pm$ 0.1mJ pulse, 9.5keV X-rays measured by Claudiu Stan et al.[3]

YZ-plane of the three hydrogen droplets 3D simulation at 7ns. The right image shows the same view through the droplet but for the experimental data of water droplets [3]. The data shows a disk-shaped expanding cloud that is similar to the symmetric expansion (ring) shown in our simulation. Even though the droplets modeled and the droplets measured are made of different materials and have different lengths, timescales, photon energies, etc., they exhibit similar features.

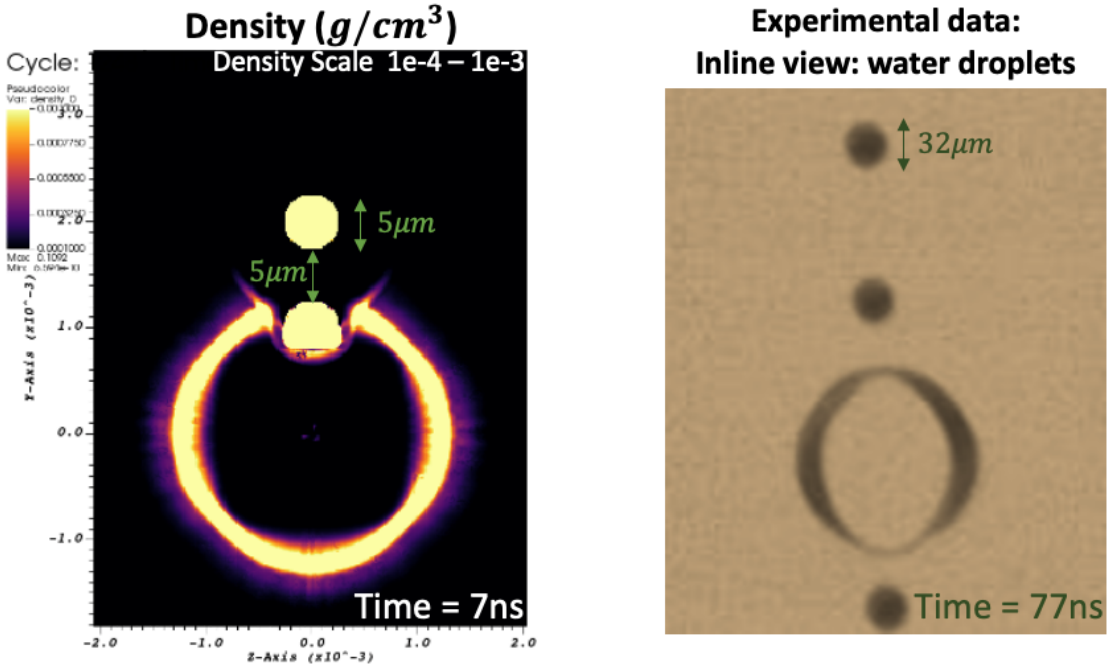

Figure 8: Inline view of droplets heated by XFEL. Top left image shows x-axis projection of 5-μm-diameter hydrogen droplets simulation after 7ns of XFEL-droplet interaction. Right image shows data measured by Claudiu Stan et al [3] of 32-μm-diameter water droplets, 1 $\pm$ 0.1mJ pulse, 9.5keV X-rays

4 Conclusion and Future Work

Initial results of multiple hydrogen droplets 3D simulations show that nearby droplets are impacted after first droplet explosion. If we had the same conditions in an experiment, this would cause a reduction in

data quantity. We see structures forming in our simulation that agree with the available experimental data for water droplets. This gives a good indication that our simulation is valid to model the real dynamics happening during the actual experiments. The next step is going to be running the PISALE code using water instead of hydrogen with the appropriate dimensions such that we can use the experimental data to benchmark the code. Future work also includes adding surface tension to the droplets. We expect that adding surface tension to the simulations will not significantly increase the runtime of the PISALE simulations [7].

5 Acknowledgements

We would like to thank many additional members of the PISALE team for their expertise and assistance throughout all aspects of our study and for their help in writing this manuscript. The PISALE code is supported by the National Science Foundation, under Office of Advanced Cyber Infrastructure Award Number 2005259, the U. S. Department of Energy, Office of Science, under Fusion Energy Sciences Research Division Award Number DE-SC0021374 and FWP100182, and the Office of Naval Research, under ONR MURI Award Number N00014- 20-1-2682. This research used resources of the National Energy Research Scientific Computing Center (NERSC), a U.S. Department of Energy Office of Science User Facility located at Lawrence Berkeley National Laboratory, operated under Contract No. DE-AC02-05CH11231 using NERSC awards ERCAP0020882 and ERCAP0020890.

References

[1] Tammy Ma, Derek Mariscal, R Anirudh, T Bremer, BZ Djordjevic, T Galvin, E Grace, S Herriot, S Jacobs, B Kailkhura, et al. Accelerating the rate of discovery: toward high-repetition-rate hed science. *Plasma Physics and Controlled Fusion*, 63(10):104003, 2021.

[2] I Prencipe, J Fuchs, S Pascarelli, DW Schumacher, RB Stephens, NB Alexander, R Briggs, M Büscher, MO Cernaianu, A Choukourov, et al. Targets for high repetition rate laser facilities: needs, challenges and perspectives. *High Power Laser Science and Engineering*, 5, 2017.

[3] C. Stan, D. Milathianaki, and H. et al. Laksmono. Liquid explosions induced by x-ray laser pulses. *Nature Physics*, 12(5):966–971, 2016.

[4] JB Kim, S Göde, and SH Glenzer. Development of a cryogenic hydrogen microjet for high-intensity, high-repetition rate experiments. *Review of Scientific Instruments*, 87(11):11E328, 2016.

[5] Alice Koniges, Nathan Masters, Aaron Fisher, David Eder, Wangyi Liu, Robert Anderson, David Benson, and Andrea Bertozzi. Multi-material ale with amr for modeling hot plasmas and cold fragmenting materials. *Plasma Science and Technology*, 17(2):117, 2015.

[6] W. Liu, A. Koniges, K. Gott, and D. Eder. Surface tension models for a multi-material ale code with amr. *Int Computers and Fluids*, 151:91–101, 2017.

[7] J. McKee, Y. Mileyko, A. Fisher, and A. Koniges. Developing a modern cfd framework with parallel algorithms and mesh adaption. *International Conference on Computational Fluid Dynamics (ICCFD11)*, 2022.

[8] S. M. Seltzer. Calculation of photon mass energy-transfer and mass energy-absorption coefficients. *Radiat. Res*, 136:147–170, 1993.

[9] S. et al Neppl. Attosecond time-resolved photoemission from core and valence states of magnesium. *Phys. Rev. Lett*, 109:087401, 2012.

[10] B.L. Henke, E.M. Gullikson, and J.C. Davis. X-ray interactions: Photoabsorption, scattering, transmission, and reflection at e = 50-30,000 ev, z = 1-92. *Atomic Data and Nuclear Data Tables*, 54(2):181–342, 1993.